New suspension system for the gravitational wave bar detector AURIGA

Michele Bignotto
Department of Physics, University of Padova and INFN Padova, via Marzolo 8, I-35100 Padova, Italy

Michele Bonaldi
Istituto di Fotonica e Nanotecnologie CNR-ITC and INFN Trento, I-38050 Povo (Trento), Italy

Massimo Cerdonio and Livia Conti
Department of Physics, University of Padova and INFN Padova, via Marzolo 8, I-35100 Padova, Italy

Francesco Penasa and Giovanni A. Prodi
Department of Physics, University of Trento and INFN Trento, I-38050 Povo (Trento), Italy

Gabriele Soranzo, Luca Taffarello,[a] and Jean-Pierre Zendri
INFN Padova Section, via Marzolo 8, I-35100 Padova, Italy

(Received 14 March 2005; accepted 30 May 2005; published online 21 July 2005)

We report on the design of the new suspension system for the gravitational wave bar detector AURIGA. The system was designed with the aid of finite element modeling simulations with the goal of achieving at least −240 dB of vibration reduction at 900 Hz in a cryogenic environment, while preserving a high mechanical quality factor. We report room temperature measurements of the suspension core stage, mode frequencies, and attenuation and we discuss them on the basis of the simulation predictions. The suspension system is currently installed in the detector, which is properly working at the operating temperature of 4.2 K. The observed improvements related to the suspension design are reported and discussed. © *2005 American Institute of Physics.*
[DOI: 10.1063/1.1988107]

I. INTRODUCTION

AURIGA is a gravitational wave (GW) bar detector at the Legnaro National Laboratories of INFN in Italy: it operated continuously in the years 1997–1999 and the collected data, analyzed in coincidence with that from the others distributed worldwide, running GW detectors, has allowed one to set upper limits to the flux of GW impinging on the Earth.[1] AURIGA consists of a 2.3 ton, 3-m-long aluminum cylinder (hereafter referred to as the bar), whose first longitudinal mode resonates at about 920 Hz. The GW acts as a driving force for this mode and the detection strategy is to monitor its dynamics: the bar motion is read by a resonant capacitive transducer fixed at the bar end face. The bar is kept at cryogenic temperatures in order to minimize the thermal noise excitation of the mode and is horizontally suspended from a cascade of mechanical filters to reduce the mechanical noise. In the run 1997–1999 the suspension design was based on a room temperature stage formed by rubber stacks and followed by a cascade of four pendula, each formed by a Ti cable suspending a shell made of aluminum or copper. The last stage of the suspension was a belly Cu cable which supported the bar at its middle section. The shells of the mechanical filters acted as thermal radiation shields: in AURIGA the mechanical suspension and the cryogenics were deeply interconnected. The total isolation was −240 dB at 920 Hz; the bar temperature was kept between 4 and 0.1 K by means of a helium bath and a He^3–He^4 dilution refrigerator. The detector setup of the run 1997–1999, including the suspension, is fully described elsewhere.[2]

In the second run of AURIGA[3] a main readout upgrade was planned, to increase the detector bandwidth from few Hz to 100 Hz. The suspended shell's design does not allow one to obtain such a wide frequency range completely free from suspension resonant modes, so that we designed a brand new suspension. A geometry constraint in the design was the need for fitting in the same cryostat as the previous run and the presence of the refrigerator inserted at the center of the apparatus, from the top. This article describes the design, modeling, and testing of the new mechanical suspension.

II. SUSPENSION REQUIREMENTS AND DESIGN

Ground motion at the AURIGA site was measured in the range $1-10^3$ Hz.[4] We found a good agreement with general characteristics observed worldwide: spectral amplitudes are of the same order of magnitude in all three orthogonal space directions, and displacement amplitude spectra follow within one order of magnitude the empirical power law:[5]

$$\sqrt{S_{ss}(f)} = \frac{\beta A}{f^2} \frac{\mathrm{m}}{\sqrt{\mathrm{Hz}}}, \tag{1}$$

where $A = 10^{-7}\ \mathrm{m/s^2\sqrt{Hz}}$. The numerical coefficient β depends on the human activity level and ranges from $\beta \sim 1$, on Sundays, up to $\beta \sim 10$ on weekdays.

After these preliminary considerations, the requirements on the suspension performances can be summarized as follows.

R1—Attenuation: The target sensitivity of the AURIGA

[a]Electronic mail: luca.taffarello@lnl.infn.it

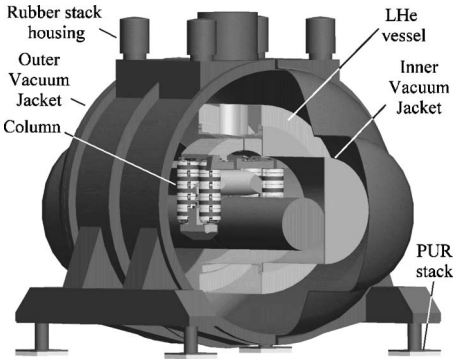

FIG. 1. AURIGA detector, partially sectioned to show the toroidal liquid helium vessel, the thermal shields, the suspension system, and the bar. The column assembly represents the core of the new AURIGA suspension and is described in detail in the text. The thermal shields are not shown for clarity. The total height of the cryostat is about 4 m.

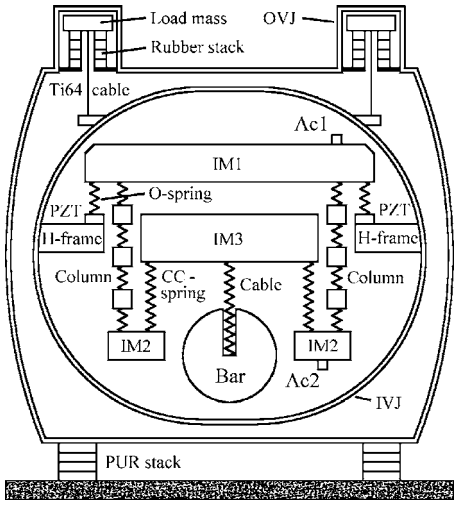

FIG. 2. Schematic view of the suspension system (not drawn to scale). The outer vacuum jacket (OVJ) is supported in four points by a layer of polyurethane (PUR) foam. The OVJ weighs about 9 tons, but the total static load on the foam is the weight of the complete detector, about 22 tons. The inner vacuum jacket (IVJ) weighs 3 tons and is supported by four cables, each suspended by a rubber stack loaded by a 50 kg mass. The IVJ and all the parts inside are at cryogenic temperature. The position of the excitation piezoelectric ceramics (PZT) is shown, as well as the accelerometers (AC1 and AC2) used in the attenuation measurement. The inertial masses IM1 and IM3 weigh, respectively, 140 and 127 kg. The load mass of each stage of the column weighs 26 kg, while each mass IM2 weighs 52 kg. The aluminum bar weighs 2.3 tons.

detector, when cooled down to 0.1 K, is some 10^{-22} m/$\sqrt{\text{Hz}}$ in a 100 Hz bandwidth centered around 900 Hz. From Eq. (1) the seismic noise at 900 Hz is at worst $\sim 10^{-12}$m/$\sqrt{\text{Hz}}$; then the overall reduction of the vibration of the suspension point of the bar should be better than −200 dB. In order to allow some maintenance activity on the operating detector we require a target of −240 dB isolation in the detector bandwidth. We point out that vertical and horizontal isolation are both required. In fact horizontal vibrations of the suspension point drive easily the longitudinal mode of the bar. On the other side vertical oscillations can force the longitudinal mode by the compression of the material in the suspension point. The efficiency of this conversion is of the order of 0.3, namely the Poisson module of the bar's material.[6]

R2—Quality factor: The new suspension must not spoil the mechanical quality factor of the bar, which was indirectly estimated as 7×10^6 in the AURIGA first run. Then, to avoid dissipating effects from residual coupling, the suspension stages close to the bar must be made of high quality factor materials.

R3—Internal modes frequency: The suspension should be free from resonant modes in a broad frequency range centered on the bar resonance (about 900 Hz). In fact any suspension resonance would amplify the mechanical noise thus reducing the suspension gain. Moreover the suspension modes could couple with the bar modes and contribute with their thermal noise to the detector overall noise.

R4a—Ultracryogenic (0.1 K) compatibility: The suspension must allow a proper cooling of the detector down to 100 mK. Any direct connection from the mixing chamber of the dilution refrigerator, and/or from the liquid helium bath, must obviously be avoided: a cooling path to the bar fully integrated with the suspension must be provided. In order to cool down the bar in a sufficiently short time and to avoid large thermal drifts of the base temperature, this link must have thermal conductance much larger than the bar intrinsic one. A simple evaluation allows one to set the minimal requirements for the suspension thermal conductivity as 2 mW/K at 0.1 K.[7,8] The experimental facts this analysis is based on are: (a) a negligible power is dissipated in the readout, (b) the readout wirings (signal and control) are directly thermalized on the mixing chamber and do not give any additional input power on the bar, (c) the residual input leak on the bar is less than 10 μW at 100 mK.

R4b—Cryogenic (4.2 K) compatibility: The analysis of the thermal properties of the detector, supported by the data collected in the AURIGA first run, shows that the bar must be connected to the helium bath by a thermal link with a conductivity better than 2 mW/K at 4.2 K. Notice that this requirement is more easily achievable than R4a as the thermal conductivity (below 4.2 K) is essentially proportional to the temperature: an "R4a compliant" thermal link (2 mW/K at 0.1 K) will raise its thermal conductivity to about 100 mW/K at 4.2 K. Then a cryogenic (4.2 K) operating temperature can be obtained by a simpler suspension configuration.

R5—Vacuum compatibility: AURIGA needs a vacuum of 10^{-6} mbar to prevent discharging of the capacitive readout which monitors the bar motion and which is biased by an electric field of the order of 10^7 V/m. The use of optical readout would impose a similar requirement, to avoid the noise induced by refraction index fluctuation of the residual gas. For this reason the suspension internal to the cryostat inner vacuum jacket (IVC) cannot have parts in rubber.

R6—Yield strength: In the old suspension design stress values as high as 60% of the yield strength were applied to the belly OFHC Cu cable, which supported the bar at its middle section. To limit the possibility of not-modeled noise caused by creep in the stressed materials,[9] we adopt a very conservative design and do not exceed 25% of yield strength in any suspension elements.

The transfer function of a simple spring-mass oscillator

TABLE I. Mechanical properties of the materials used in the suspension. If low temperature data for the specific metal were not available, the indicative properties of the alloy family is given. Young modulus at 4.2 K raises at low temperature by about 10% for the listed materials, causing a 5% modes frequency increase. The yield stress of stainless steel and titanium considerably raises at low temperatures, increasing the design confidence. On the other side the yield stress of copper alloys remains essentially unchanged at cryogenic temperatures. As the yield strength of the annealed copper temper is very low and quite unpredictable, we avoided the use of this material in structural parts.

Material	Suspension element	Density (ton/m^3)	Young modulus (GPa) 300 K	Yield stress R_p 0.2 300 K (MPa)	Yield stress R_p 0.2 4.2 K (% raise)
AISI 316L[a,b]	H frame	8.0	190–200	205	>100%
Ti 6Al 4V[c]	O spring	4.45	114	830	100%
Al 2017A T452 (2xxx series aluminum-copper)[b,d]	IM1, IM2	2.71	71.5	275	25%–35%
Alumold 1-500 T652 (7xxx series aluminum-zinc)[b,d]	C spring, CC spring	2.82	72	532	25%–35%
Al 5056 (5xxx series aluminum-magnesium)[b]	IM3, bar	2.71	70	315	30%–40%
Cu–Be C17200[b,e]	Cable-cryogenic	8.8	117	1138	20%–30%
OFHC Cu C10200 $\frac{1}{4}$ hard (H01)[e,f]	Cable-ultracryogenic	8.8	117	260	15%–20%
OFHC Cu C10100 cryogenic grade (annealed)[e,g]	T spring	8.8	117	30–110	15%–20%

[a]Reference 12.
[b]Reference 15.
[c]Reference 16.
[d]Reference 17.
[e]Reference 18.
[f]Reference 19.
[g]Reference 20.

(with K the elastic constant, M the mass, $2\pi f_0=\sqrt{K/M}$, Q the quality factor) driven by a vibration of its suspension point is

$$T_{HQ}(f)=\frac{f_0^2}{f_0^2-f^2} \tag{2}$$

in the high quality factor case ($f_0Q \gg f \gg f_0$), and reduces to

$$T_{LQ}(f)=\frac{f_0}{Qf} \tag{3}$$

in the low quality factor case ($f \gg Qf_0$). To enhance the attenuation efficiency, the suspension must be made by a cascade of simple harmonic oscillators, the total isolation given by adding the isolation of each stage, properly evaluated according Eq. (2) or (3).

The design of the AURIGA cryostat[10] is more than 15 years old and was produced without the aid of FEM methods. For this reason the cryostat and the helium vessel display many resonant modes within the upgraded detector bandwidth. As we could not completely redesign our apparatus to avoid this problem, we fulfill the −240 dB isolation (requirement R1) by the use of six suspension stages, designed to operate at cryogenic temperatures, assembled in columns and housed inside the IVJ together with the bar (Fig. 1). The inner cryogenic stages will act not only against external noise sources (such as human activity, seismic and acoustic noise) but also against internal noise sources, like the boiling of cryogenic liquids and the possible acoustic emission by highly stressed components due to thermal contractions.

Requirement R2 forces the use of high quality factor materials for the cryogenic suspension stages, as they are installed near the bar. Their fundamental resonances are placed at relatively high frequencies (40–90 Hz), if compared with the first AURIGA run, when the cryogenic suspension stages were resonating in the 2–10 Hz range. This choice should reduce the seismic noise drive of large oscillations of the fundamental resonances, as the seismic noise is significantly lower at higher frequency [see Eq. (1)]. At high frequency we can also profit from some preliminary attenuation provided by two low frequency stages of the suspension, one located in air and one inside the outer vacuum jacket (OVJ).

Requirement R3 made it necessary to fully separate any thermal shell from the suspension, as the shells display many modes in the detector bandwidth. The volume constraint results in the suspension not simply hanging from the bottom: to gain vertical space the presence of inverted stages (i.e., stages where the top is quieter than the bottom) is necessary. Figure 2 shows a schematic view of the suspension topology; the terms defined there will be useful for the following system description.

The suspension was designed with the aid of the commercial software PRO/ENGINEER.[11] Static and modal analyses were obtained by the commercial software PRO/MECHANICA,[11] which is a finite element modeling (FEM)

program which interacts directly with PRO/ENGINEER. The described analysis is based on room temperature material properties (Table I). Notice that the yield stress of titanium and aluminum increases considerably at cryogenic temperatures, increasing the confidence both on the design and on the requirement R6. Young modulus of the employed materials raises by about 10%,[12] so that the frequency of the resonant modes is expected to increase by about 5% at low temperature.

A. Low frequency preliminary stages

It is very difficult to evaluate and to measure the isolation ratio of the low frequency suspension stages, because their effective inertial mass is strongly dependent on the frequency: the OVJ shell and the IVJ shell (which integrates the helium vessel) are large solid bodies with a number of resonant modes below 1 kHz, which couples in an unpredictable manner and induces steep changes in the isolation factor. For this reason the low frequency stages design goal is essentially to reduce the seismic noise amplification by the internal modes of the OVJ and IVJ. A strong damping is then provided by the use of rubber materials, which are allowed as the vacuum compatibility requirement R5 only applies to the IVJ. We measured an isolation ratio in the -10 to -40 dB range in the detector bandwidth, which we consider satisfactory, as the degree of isolation needed for the detector is fulfilled by the following cryogenic stages of the suspension.

As shown in Figs. 1 and 2, the whole AURIGA cryostat is supported in four points by a layer of a highly dissipative polyurethane foam (PUR).[13] The cutoff frequency of this first passive mechanical filter is about 10 Hz and its quality factor is less than 2.

A second low frequency stage is then formed by four titanium cables supporting the liquid helium vessel from the OVJ. As clearly shown in Fig. 2, the cables are suspended through a rubber stack,[14] providing both vertical vibration attenuation and the necessary amount of damping. Each stack is loaded by a Pb mass of about 50 kg to improve its isolation performances. The cables are made in Ti64, have a diameter of 11 mm and a length of 2.3 m. The helium vessel supports the other parts of the IVJ, the high frequency isolation system and the bar. The cables' assembly also gives the required thermal isolation to the vessel and comes from the first AURIGA run.

B. Cryostat interface and inertial reference

In order to fit the new suspension inside the cryostat it was necessary to design an H-shaped frame (Fig. 3) attached on one side to the helium dewar and supporting on the other the new suspension and the three inner thermal shields: this is the only contact point between suspension and shields. One additional benefit is that now the shields can be much lighter (thus shortening the cooling time) than in the previous run, when the shield masses were chosen in order to optimize the transfer function of the mechanical filters. This H frame is made out of stainless steel: the material is chosen to be identical to the one of the helium tank, which it is in thermal contact with, so to avoid dangerous differential contractions during the cooling.

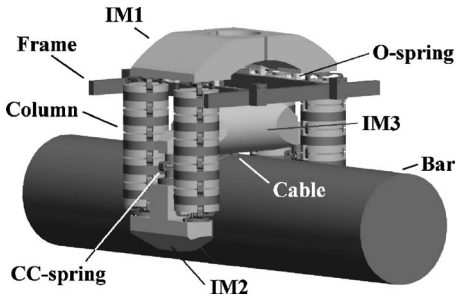

FIG. 3. Detail of the suspension system. The stainless steel H frame (130 kg in mass) is attached to the helium dewar and supports the inertial mass IM1 by the four compression O springs. The mass IM1 (140 kg) measures $1016\times550\times216$ mm. The columns are 775 mm height and their diameter is 250 mm. A column is obtained by assembling five identical C-spring stages, each loaded with a 26 kg total mass, made of six brass pieces assembled in a space-saving design. The lowest C-spring stage is loaded by the inertial mass IM2. The inertial masses IM2 then support the inertial mass IM3 by the two compression CC spring. Each mass IM2 (52 kg) measures $600\times370\times180$ mm, while IM3 (127 kg) measures $300\times300\times1020$ mm.

The suspension is then mechanically isolated from its supporting H frame by a set of four springs (O springs) connecting the frame to an inertial mass IM1 which the suspension is hung to. These are compression springs dimensioned so to guarantee -20 dB of isolation ratio at about 1 kHz and to support each a load of 10 kN; the material is chosen to be Ti 6Al 4V. The central hole on the inertial mass (Fig. 3) allows the insertion of the dilution refrigerator, to be used in the third AURIGA run. The O springs are attached to the H frame at nodal points of the frame modes resonating at about 1 kHz. These nodal points are determined by running a full simulation of the structure and are a compromise between the nodal points of several modes in the range 600–1300 Hz. The inertial mass IM1 acts as reference plane for the suspension: it is designed not to have internal modes in the frequency range between 400 and 1500 Hz and to be in thermal contact with the 1Kpot of the dilution refrigerator. According to Table I, the material is chosen to be an aluminum alloy (Al2017A) which has a good yield stress over density ratio and a good thermal conductivity above 1 K; the mass is 140 kg. The assembly of the H frame, O springs, and inertial mass is obtained by means of screws. The FEM simulation indicates that there are no modes of the inertial mass from 620 to 1250 Hz; the simulation shows also that, at full load, the stress on the springs stays below 25% of the yield stress. As frame and inertial mass will work at different temperatures (respectively, 6–10 and 1.2–2 K), the springs are sandwiched between two layers of thermal insulator, namely Teflon™: each layer is 3 mm thick and its surface is dimensioned so that it is subject to a load 1/4 of the yield stress.

C. The columns

The use of four columns is chosen to allow the insertion of the dilution refrigerator at the center of the cryostat in the third AURIGA run and for simplicity and symmetry reasons

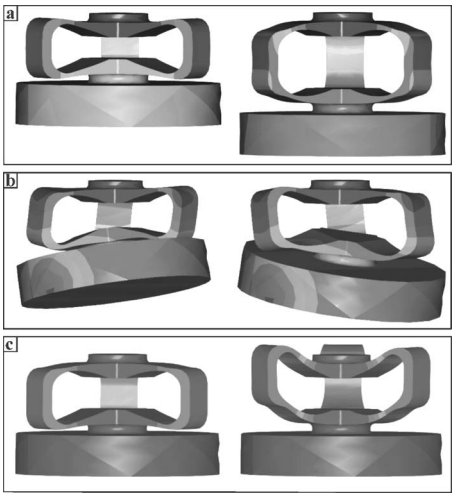

FIG. 4. Some of the C-spring fundamental modes. The modes (a) and (b) are spring-mass modes resonating below 100 Hz. They contribute to determine the performances of the isolation stage, according to Eq. (2). Mode (c) is an internal spring-mode resonating at about 1700 Hz.

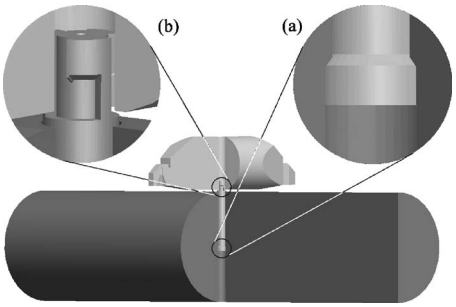

FIG. 5. Detail of the cable suspension. The bar (sectioned) is supported from its center of mass, through a central hole with a diameter of 65 mm in the bottom radius and 55 mm in the top radius. The cable is inserted from the bottom and supports the bar by a circular, conic housing [detail (b)]. The cable top end extends about 60 mm from the bar surface and is fixed to the inertial mass IM3 (sectioned) by a bayonet coupling [detail (a)]. The cable (total length 390 mm) was designed with the minimum length possible: the bayonet coupling on the IM3 is at a distance of 33 mm from the top surface of the bar. The resulting distance between the IM3 and the bar is about 11 mm.

(Fig. 3). This stage of the suspension is asked to fulfill by itself the required isolation (at least −240 dB at 1 kHz). Each column consists of a set of six stages, each providing an isolation ratio of −40 dB at 1 kHz: according to Eq. (2), this condition sets the upper limit to the stage resonance at 100 Hz. In order to satisfy the requirement R3, no internal modes should be present in the frequency range 500–1500 Hz. We point out that this requirement could not be satisfied by the AURIGA first run cable suspensions, due to the presence of a large number of violin modes and thermal shell modes.

Each stage is made by a spring-mass system, where the use of C-shaped springs allows the design of an isolation stage with the same performances for noise vibrations directed along the three axis. This is obtained by requiring the spring to have the same elastic stiffness when pressed along any direction. Figure 4 shows the fundamental modes of a single mass-spring system stage, called C spring. Each stage consists of a number of three C-shaped springs, loaded by a mass of 26 kg, needed to maintain the fundamental modes below 100 Hz. The C-spring internal modes are all above 1700 Hz, while the mass is designed to have internal modes above 2 kHz.

In the design and in the material choice we also took care not to introduce high stresses to avoid creep. Each spring assembly is machined from a single piece of a special aluminum alloy, named Alumold 1-500 T652 (Table I): the maximum applied stress is lower than 25% of the yield stress. Also care was taken that during the machining the material was subject to a minimum mechanical stress. The several pieces are assembled together by means of Al7075 alloy screws, dimensioned so that the torque to be applied corresponds to 15% of the yield stress of the Al7075.

D. Last stage and suspension cable

At this point no further isolation degree is required and these suspension components are only needed as adapting pieces between the columns and the bar.

The columns are paired by joining them to two load masses IM2, which also act as load masses for the last stage of the column (Fig. 3). These masses, made out of the same material as the inertial mass IM1 which the columns are hanged to, do not have resonant modes below 2 kHz. The IM2 masses support the inertial mass IM3 by means of a couple of compression springs, called CC springs. The latter have no requirements on the isolation, except for the absence of internal modes in the frequency range 500–1500 Hz. The material is the same as C springs, the shape is also similar except for the thickness, as CC springs are double loaded with respect to C springs. We avoided screws to fix the mass IM3 to these springs in order not to introduce possible source of creep near the bar and not to lower its mechanical quality factor. A conic housing blocks mass IM3 to the springs. The simulation indicates that the springs have a vertical mode at about 310 Hz and that the applied stress is lower than 10% of the yield stress. The CC springs lateral stiffness is properly dimensioned to avoid any system instability, potentially introduced by the inverted pendulum configuration used in these suspension stages.

The inertial mass IM3 plays an important role as the bar is thermally anchored to it and it is also the stage where the cable is fixed before reaching the bar. Due to its closeness to the bar, IM3 needs to have high mechanical quality factor. We decided to machine it from a single piece of the same aluminum alloy as the bar, namely Al5056. At the center a hole is present to hang the cable that supports the bar. Again, no screws are present: the cable is fixed by means of a bayonet coupling. The simulation indicates that the first mode is at about 1600 Hz.

The cable that supports the bar is the last stage of the suspension: it must guarantee enough thermal conductivity at cryogenic temperatures and not introduce resonances in the detector bandwidth due to its acoustic modes. The material quality factor must be high to preserve the one of the bar. As shown in Fig. 5, in order to support the bar from its center of mass, we had to cut a central hole in the bar. The cable is inserted from the bottom and supports the bar by a circular,

TABLE II. Thermal conductivity data for the materials used in the suspension. As it is not uncommon to have large uncertainties (Ref. 23), a very conservative design was adopted in the suspension thermal modeling. The poor thermal conductivity performances of structural spring materials (titanium alloy, aluminum alloys, Cu–Be alloy) enforce the use of OFHC copper for the ultracryogenic thermal path. Notice that the 0.1 K conductivity data for aluminum and titanium based alloys refer to the normal state of the material; in the superconducting state their thermal conductivity is expected to be two orders of magnitude lower. The thermal conductivities of the OFHC copper samples are estimated on the basis of their RRR (Ref. 25).

Material	Suspension element	Thermal conductivity (W/(K m)) 100 K	4.2 K	0.1 K
AISI 316L Stainless steel[a,b]	H frame	8–10	0.2–0.3	$<10^{-2}$
Ti 6Al 4V[c]	O spring	3–4	0.1–0.2	$<10^{-2}$
Aluminum alloys[d,e]	IM1, IM2, IM3, Bar, C spring, CC spring	50–90	3–5	$<10^{-3}$
Cu–Be C17200[f]	Cable—cryogenic	40	1–2	0.4–0.7
OFHC Cu C10200 $\frac{1}{4}$ hard (H01) $(50<\mathrm{RRR}<100)$[g–i]	Cable—ultracryogenic	400	250–500	8–13
OFHC Cu C10100 cryogenic grade $(300<\mathrm{RRR}<400)$[j]	*T* spring	400	1500–2000	30–40

[a]Reference 21.
[b]Reference 22.
[c]Reference 23.
[d]Reference 8.
[e]Reference 17.
[f]Reference 24.
[g]Reference 18.
[h]Reference 19.
[i]Reference 23.
[j]Reference 20.

conic housing on the end. The surface of the conic housing on both ends is dimensioned in order not to exceed the load of 50 $\mathrm{N/mm^2}$ when the bar is suspended. This way both the IM3 mass and the bar are loaded no more than 20% of the Al5056 yield stress. We point out that both ends of the cable are fixed without the aid of screws, which introduce mechanical losses in our experience.

The new suspension design allows a very rigid design for the cable: the belly cable used in the previous AURIGA run had a 78 $\mathrm{mm^2}$ section, while our cable can reach a section as large as 2100 $\mathrm{mm^2}$. The cable performances represent a compromise between two opposite requirements, high yield stress and high thermal conductivity, and both of them can be now more easily satisfied as large sections are employed. We then realized two cables, one made of Cu–Be and the other of OFHC copper, to be used as mutually exclusive options depending on the target working temperature of the detector (see Sec. III).

The Cu–Be cable is the best choice from the mechanical point of view, on the other side its thermal conductivity is very low. It is actually a hollow cylinder with diameter 44 $\times 52$ mm (section 600 $\mathrm{mm^2}$), free of resonant modes below 1200 Hz, loaded at about 5% of its yield stress. The OFHC copper cable is a full cylinder with outer diameter 52 mm (section 2100 $\mathrm{mm^2}$), free of resonant modes below 1100 Hz, and made of a Cu alloy specifically chosen (see Table I) in order to load less than 20% of the yield stress and to allow the proper cooling of the bar.

III. DETECTOR COOLING

By the use of high strength materials quite low yield stress values were obtained in the suspension spring elements. Unfortunately these materials perform poorly as thermal conductors, so that the cooling requirements of the detector have to be verified carefully and proper thermal links must be designed where necessary, in order to satisfy requirements R4.

The thermal design is based on the thermal conductivity of the materials at cryogenic and ultracryogenic temperatures (see Table II). These values are strongly dependent on the sample composition, its thermal treatment and in some cases the mechanical stresses applied during the machining. For our purposes the approximated results obtained by the use of tabulated conductivity data are acceptable, and the possible systematic errors are simply prevented by a conservative design. For this reason we considered redundant the precision offered by a full thermal design by FEM.

A. Cryogenic cooling

If a cryogenic (4.2 K) operating temperature is required for the detector, no additional thermal links must be attached to the suspension to cool down the bar. In this case the inertial mass IM1 is thermalized directly to the liquid helium bath by an high conductivity multi-wire OFHC copper link, 150 mm long and of 200 $\mathrm{mm^2}$ total cross section, with an expected thermal conductivity of 0.4 W/K. The suspension

system conductivity is essentially limited by the columns and by the cable, as the inertial masses (IM1, IM2, and IM3) have much larger cross section.

The thermal conductivity of the columns at 4.2 K is about 10 mW/K, as given by the C springs equivalent length (1.5 m) and section (5×10^{-3} m^2). The Be–Cu hollow cable (600 mm^2 section, 300 mm long) then sets the thermal path conductivity limit to about 3 mW/K. This value satisfies our requirement R4b and allows the normal operation of the AURIGA detector down to 4.2 K. Notice that while the power dissipated in the capacitive readout is very low, some unfrequent calibration procedure dissipates as much as 80 mW for a time 400 s long. In this case the bar temperature will drift up to 0.2 K and the detector operation will have to be stopped for some hours.

B. Ultracryogenic cooling

When a 100 mK working temperature is required, a high conductivity thermal path is needed to allow the proper cooling of the 2.3 ton aluminum bar. A thermal conductivity of 2 mW/K (requirement R4a) allows one to cool down the bar in a few hours from 4.2 K and to avoid large thermal drifts of the base temperature. At the temperature of 100 mK the thermal conductivity of the suspension elements (both springs and masses) is well below this value: a separate cooling path must be added to the suspension, providing an uninterrupted link from the dilution refrigerator mixing chamber to the bar.

This path cannot be simply obtained by some kind of flexible connection running along the suspension chain: specific spring-like elements had to be developed and fully modeled with the suspension elements which they are coupled to. Our basic element consists of properly dimensioned copper rods, soldered together to obtain C-shaped T springs free from vibrational modes in the 300–1500 Hz range. As the T spring is much softer than the springs used in the suspension system (O springs, C springs, or CC springs), it can be used as a "bridge" across any stage (as shown in Fig. 6 in the case of a column) without spoiling off its isolation performances (i.e., the spring-mass fundamental mode frequencies are not modified). T spring are not dimensioned to support any weight and must be anchored to the suspension only when it is fully loaded.

The T springs must be made by a "cryogenic grade" OFHC copper (see Table II), specially developed to be used in composite superconducting wires[20] and available with residual resistance ratio at 4.2 K (RRR) values up to 500. The full chain thermal conductivity at 100 mK is at least 1 mW/K, and two parallel chains must be used in order to satisfy the requirement R4a. On the other hand the cable material choice is less demanding in terms of thermal conductivity: thanks to its section as high as 2100 mm^2, a thermal conductivity of 42 mW/K at 100 mK can be obtained with the cold worked (H01) OFHC copper described in Table I. We point out that RRR values in the 50–100 range are easily found in this OFHC copper but are not guaranteed by the alloy specifications. The RRR of our specific samples must then be verified before being installed in the detector.

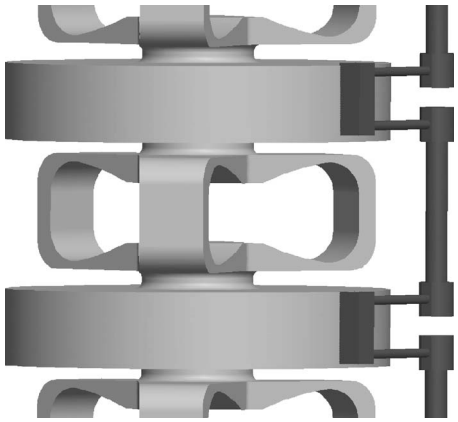

FIG. 6. Detailed view of the cooling path attached to the column. The T-springs thermal conductivity is essentially determined by their horizontal segment (6 mm outer diameter, 65 mm long) with 30 mm^2 cross section. A complete thermal link from the inertial mass IM1 to the OFHC copper cable is obtained by chaining seven T springs; the parts must be vacuum brazed to maintain their thermal conductivity. Two parallel links must be used to obtain the required thermal conductivity. T springs made by stainless steel tubing can be used to realize a cold gas closed circuit for the detector precooling.

C. Preliminary cooling

The preliminary detector cooling (from room temperature down to liquid helium temperature) cannot be simply made by a thermal path. In this case about 400 MJ must be extracted by the bar and a cooling power of at least 200 W is needed to maintain the cooling time within a few weeks. The preliminary AURIGA detector cooling is accomplished by inserting some He gas (10^{-1} mbar) into the vacuum chamber housing the bar: the gas shorts thermally the helium bath with the experimental apparatus.

This exchange gas procedure can introduce or displace dust inside the vacuum chamber and is dangerous for the capacitive readout element. Moreover the residual gas sensitivity of the cryogenic Fabry-Perot cavities prevents the use of our new optical readout. For this reason we designed a closed flow circuit embedded in the suspensions, allowing for a forced cold gas flow to be used as an alternative preliminary cooling. We stress that the use of the cold gas flow is not aimed at speeding up the cooling procedure, as recently obtained by blowing a cold flow against a 1.2 ton detector.[26]

Our gas circuit is essentially made by stainless steel tubing, 5 mm inner diameter, arranged in a T springs design for a total length of about 5 m. The circuit has the same dimension as the thermal path shown in Fig. 6 and is anchored to a column in the same way. The cold end of the circuit is in good thermal contact with the OFHC cable supporting the bar, connected at the cable's top head by a single M10 screw. A bellows system (10 mm inner diameter, 5 m total length) is used to continue the cold gas flow outside the cryostat. A flow of 0.5 mol/s can be easily precooled by a liquid nitrogen heath exchanger and then forced through the circuit, providing the required 200 W cooling power at the bar.

TABLE III. Simulated and measured mode frequencies of a single C-spring stage loaded with its design mass. The agreement with the simulation is good and no unexpected resonant modes were found below 2000 Hz.

Mode	FEM frequency (Hz)	Measured frequency (Hz)
1	38±2	38.8
2	39±2	40.0
3	75±4	74.2
4	86±3	82.5
5	86±2	86.9
6	87±3	87.7
7	1850±50	1815.0

IV. RESULTS

A. Modal analysis

A modal simulation of the full isolation system and the bar does not show any vibrational mode within the detector bandwidth (850–950 Hz). Just one mode at 715 Hz of the inertial mass IM1 is present within the range 650–1200 Hz, and we consider it acceptable as it is placed before the isolation columns and then its vibrations will be attenuated sufficiently. The simulation also shows that the cooling path attached to the isolation stage does not significantly modify the frequency of the modes.

In order to verify the FEM predictions, experimental measurements were performed at room temperature to characterize the resonant modes of the core element of the isolation system, the C-spring-mass stage. The single stage, properly insulated by external acoustic and vibrational disturbance, was excited on the spring side by a piezoelectric actuator. The resonances are clearly indicated by sharp maxima in the displacement of the load mass. In Table III we list the mode frequencies resulting from the modal analysis of a single C-spring-mass stage and those found experimentally: the agreement is within 5%.

We also measured the vertical resonance of the last stage of an assembled column, in order to check that the real coupling of so many stages, each with its machinery tolerances, did not introduce unexpected vibrational modes. The complete FEM analysis of a five-stage column shows 34 modes in the range 1–2000 Hz, with a free range 170–1700 Hz. In Table IV the expected and measured vertical resonant modes of the last stage of the column are shown. The agreement with the simulation is good and no unexpected modes were observed below 2000 Hz.

TABLE IV. Expected and measured frequencies of the column modes which induce a vertical displacement of the last stage. Considering the complexity of the system (five cascaded stages of three-dimensional oscillator), we consider the experimental data in remarkably good agreement with the FEM evaluation.

Mode	FEM frequency (Hz)	Measured frequency (Hz)
6	24.9±0.5	20.1
10	73±2	68.4
20	114±3	121.6
28	146±3	139.8
30	167±3	166.2

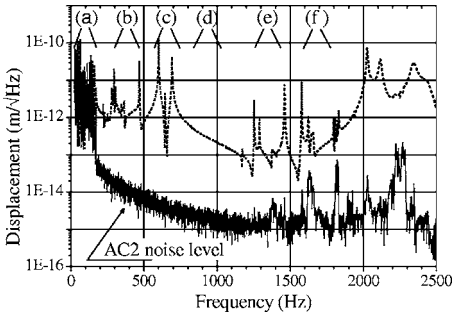

FIG. 7. Dotted line: vertical displacement of the inertial mass IM1, as measured by the accelerometer AC1 (see Fig. 2). Continuous line: vertical displacement of the inertial mass IM2, as measured by the accelerometer AC2; for most of the frequency range it remains below the accelerometer noise, which is proportional to $1/\omega^2$. On the basis of the FEM analysis, we are able to explain the peaks occurring on both curves. (a) Column modes up 180 Hz: visible both on AC1 and AC2. (b) O-spring modes: clearly visible in AC1, highly attenuated and below the AC2 resolution. (c) Lower inertial mass IM1 internal modes (650, 715 Hz): highly attenuated and below the AC2 resolution. (d) Region free by IM1 modes, centered around resonant frequency of the bar. (e) Higher IM1 internal modes (1280, 1500 Hz): highly attenuated and below the AC2 resolution. (f) C-spring column internal modes (over 1600 Hz): visible both on AC1 and AC2.

B. Vibration isolation

The filtering of the full suspension is so high that it cannot thoroughly measured by a dynamic analysis with the use of commercial sensors: only the operating detector has enough sensitivity to evaluate the overall vibration reduction. On the other hand the evaluation of the full transfer function by FEM can be problematic, as internal roundoff errors and truncation errors could affect standard FEM routines when calculating attenuation factor in the 10^{12} range. For this reason we still judged it interesting to estimate a lower limit for the isolation chain performances by a room temperature dynamic analysis.

We installed four piezoelectric actuators PZT under each O spring, as shown in Fig. 2, and applied an oscillating vertical force in the frequency range 1–2500 Hz. The resulting displacement was simultaneously measured by the accelerometer AC1 attached to the mass IM1 and by the accelerometer AC2 attached to the inertial mass IM2. The isolation efficiency of the columns can be estimated by the vibration transmission from IM1 to IM2.

The accelerometers' output is shown in Fig. 7. As described in the figure caption, many resonant modes can be identified on the basis of the FEM modal analysis. Notice that the inertial mass IM2 displacement is below the AC2 accelerometer resolution in the 200–1300 Hz range, but a lower limit on the columns' performances can be inferred by the 600 Hz IM1 mode peak, reduced by at least −140 dB. This number is consistent with the −186 dB theoretical attenuation value predictions. Moreover the measurements confirm the existence of a wide frequency range centered around the bar resonance and free by suspension resonant modes.

C. AURIGA detector run

The second AURIGA run aims at demonstrating the bandwidth and sensitivity enhancement made possible by a two-mode resonant readout. Therefore we decided to avoid any problem coming from the use of a dilution refrigerator, namely vibrational noise and duty cycle reduction. For these reasons AURIGA was cooled in December 2003 with a goal operating temperature of 4.2 K, easily obtained by the thermal conductivity of the suspension elements alone. The preliminary cooling was obtained by the use of some exchange He gas inside the inner vacuum chamber.

In the first AURIGA run (years 1997–1999) the spectral noise performance of the detector was worse than the design one. In fact the minimum noise temperature reached by the two mechanical resonators was lower bounded to 0.8 K, while their thermodynamic temperature was as low as 0.2 K.[2,27] These results were achieved for a fraction of about 30% of the data acquisition time. In addition, the measured rate of impulsive mechanical excitations on the bar was typically almost two orders of magnitude greater than the rate expected from the modeled intrinsic noise sources, which were dominated by the Brownian mechanical noise.[2] In the current operating configuration, the upgraded AURIGA detector is instead capable of operating with the design spectral sensitivity for 60% of the time. Moreover, the current rate of impulsive mechanical excitations on the bar is of the same order of the expected one from the modeled thermal noise sources, in spite of the fact that the current timing resolution (i.e., the bandwidth) of the detector has been improved by more than one order of magnitude.[3]

We point out that, despite the good isolation ratio provided by the high frequency cryogenic suspension, the presence of the low frequency preliminary stages is essential for the proper operation of the detector. In fact we observed that low frequency seismic noise was unexpectedly found to induce spurious line within the bandwidth, due to some not well understood upconversion effect. This noise spoils off the detector performances in the daytime due to the human activity, involving vehicles and machinery in the vicinity of the AURIGA site. For this reason we plan to improve our low frequency isolation by the use of a set of commercial pneumatic vibration isolators, which will provide a first stage with a 1 Hz cutoff in place of the currently used 10 Hz cutoff polyurethane stage. Notice that the detector in its previous run was not affected by this kind of noise, probably for one or both of these reasons: (a) the old suspension system, based on a pendulum chain, was much more effective in the frequency range typically affected by human activity, (b) the detector bandwidth to signals and then to spurious noises was a few Hz against the present 100 Hz.

The bar quality factor was not affected by the suspension, and the usual value 7×10^6 was indirectly[28] measured as in the previous run. We notice in the end that the suspension system is fully compatible with the future developments of the AURIGA detector. To be more specific, our design allows the cooling of the detector at ultracryogenic temperatures (100 mK) if equipped with a capacitive readout or, alternatively, at cryogenic temperatures (4.2 K) if equipped with an optical readout.[29]

In conclusion our new suspension system works satisfactorily and and suits the needs of the upgraded AURIGA detector, demonstrating the effectiveness of our design principles and methods. The suspension is expandable with different kinds of cooling path which will be simply installed in the next runs of the detector, according to the needs of the readout system, without any substantial system modification.

[1] Z. A. Allen *et al.*, Phys. Rev. Lett. **85**, 5046 (2000).
[2] G. A. Prodi *et al.*, *2nd Edoardo Amaldi Conference on Gravitational Waves*, CERN, Geneva, Switzerland, 1997, edited by E. Coccia, G. Pizzella, and F. Ronga (World Scientific, Singapore, 1998), pp. 148–158.
[3] L. Baggio *et al.*, Phys. Rev. Lett. **94**, 241101 (2005).
[4] M. Bignotto, thesis, University of Padova, 1999–2000.
[5] P. R. Saulson, *Interferometric Gravitational Wave Detectors* (World Scientific, Singapore, 1994).
[6] G. Pizzella, *Fisica Sperimentale del Campo Gravitazionale* (La Nuova Italia Scientifica, Roma, 1993).
[7] E. Coccia, V. Fafone, and I. Modena, Rev. Sci. Instrum. **63**, 5432 (1992).
[8] E. Coccia and T. O. Niinikoski, J. Phys. E **16**, 695 (1983).
[9] R. W. Evans and B. Wilshire, *Creep of Metals and Alloys* (The Institute of Metals, London, 1985).
[10] P. Astone *et al.*, Europhys. Lett. **16**, 231 (1991).
[11] Parametric Technology Corporation, Needham, MA, www.ptc.com.
[12] *Cryogenic Engineering*, edited by B. A. Hands (Academic, London, 1986).
[13] Sylodamp©, Getzner Werkstoffe GmbH, Herrenau 5, Postfach A–6706 Bürs/Bludenz, Austria.
[14] 741-436 metal-rubber disk isolator, Angst+Pfister AG, Thurgauerstrasse 66, Postfach CH-8052 Zürich, Switzerland.
[15] D. A. Wigley, *Mechanical Properties of Materials at Low Temperatures* (Plenum, New York, 1971).
[16] M. Reytier, F. Kircher, and B. Levesy, AIP Conf. Proc. **614**, 76 (2002).
[17] MIL-HDBK–5H, *Department of Defense Handbook: Metallic Materials and Elements for Aerospace Vehicle Sstructures* (U.S. Department of Defense, Washington, DC, 2003).
[18] N. J. Simon, E. S. Drexler, and R. P. Reed, NIST Monograph No. 177, 1992.
[19] F. Bertinelli *et al.*, CERN LHC Project Report 728, Geneva, 2004.
[20] Outokumpu Copper, Box 144, FI-02201 Espoo, Finland.
[21] O. V. Lounasmaa, *Experimental Principles and Methods Below 1 K* (Academic, New York, 1974).
[22] G. K. White, *Experimental Techniques in Low Temperature Physics* (Clarendon, Oxford, 1979).
[23] E. D. Marquardt, J. P. Le, and Ray Radebaugh, in *Cryocoolers 11*, edited by R. G. Ross, Jr. (Kluwer Academic/Plenum, New York, 2001), Proceedings of the 11th International Cryocooler Conference, Keystone, CO, 2000.
[24] A. Woodcraft, R. W. Sudiwala, and R. S. Bathia, Cryogenics **41**, 603 (2001).
[25] *Thermal Conductivity of Pure Metals and Alloys*, edited by O. Madelung and G. K. White (Springer, Berlin, 1991).
[26] A. de Waard, L. Gottardi, and G. Frossati, Class. Quantum Grav. **19**, 1935 (2002).
[27] J. P. Zendri *et al.*, in *Gravitational Waves*, Proceedings of the Third Edoardo Amaldi Conference (CalTech-California, 1999), edited by S. Meshkov (AIP Conference Proceedings, New York, 2000), pp. 421–422.
[28] The bar and its readout form a system of coupled oscillators. The quality factor of each element of this system is estimated as a parameter of the detector calibration procedure.
[29] L. Conti *et al.*, J. Appl. Phys. **93**, 3589 (2003).